PHYSICAL REVIEW B **90**, 121404(R) (2014)

Critical point for the canted antiferromagnetic to ferromagnetic phase transition at charge neutrality in bilayer graphene

S. Pezzini,[1,2,*] C. Cobaleda,[2,3] B. A. Piot,[4] V. Bellani,[1] and E. Diez[2]
[1]*Dipartimento di Fisica, Università degli studi di Pavia, I-27100 Pavia, Italy*
[2]*Laboratorio de Bajas Temperaturas, Universidad de Salamanca, E-37008 Salamanca, Spain*
[3]*NEST, Scuola Normale Superiore, Piazza S. Silvestro 12, I-56127 Pisa, Italy*
[4]*Laboratoire National des Champs Magnétiques Intenses, CNRS-UJF-UPS-INSA, F-38042 Grenoble, France*
(Received 27 July 2014; revised manuscript received 9 September 2014; published 22 September 2014)

We report on magnetotransport measurements up to 30 T performed on a bilayer graphene Hall bar, enclosed by two thin hexagonal boron nitride flakes. In the quantum Hall regime, our high-mobility sample exhibits an insulating state at the neutrality point which evolves into a metallic phase when a strong in-plane field is applied, as expected for a transition from a canted antiferromagnetic to a ferromagnetic spin-ordered phase. We individuate a temperature-independent crossing in the four-terminal resistance as a function of the total magnetic field, corresponding to the critical point of the transition. We show that the critical field scales linearly with the perpendicular component of the field, as expected from the underlying competition between the Zeeman energy and interaction-induced anisotropies. A clear scaling of the resistance is also found and a universal behavior is proposed in the vicinity of the transition.

DOI: 10.1103/PhysRevB.90.121404 PACS number(s): 72.80.Vp, 73.43.Nq

Bilayer graphene presents a unique energy spectrum upon the application of a perpendicular magnetic field [1,2], with different possible competing orders resulting from the large number of underlying symmetries of the system [3]. A huge experimental effort was dedicated to the identification of the insulating ground state at the charge neutrality point (CNP) in high-quality samples [4–7]. Recent theoretical [3,8] and experimental results [9] support the formation of a canted antiferromagnetic (CAF) phase in perpendicular-only magnetic fields, which results from the competition between the Zeeman energy $\epsilon_Z = g\mu_B B_{\rm tot}$ and an anisotropy energy $u_\perp$ originating from electron-electron or electron-phonon interaction at the lattice scale. Within the CAF ordering, the spin polarizations associated to the two valleys (and equivalently to the two sublattices and layers) have equal components in the direction of the magnetic field and are opposed in the perpendicular plane. The energy spectrum of the CAF phase presents a gap for both the bulk and edge excitations, which leads to the insulating transport behavior. While ϵ_Z depends on the total magnetic field, $u_\perp$ is sensitive only to the perpendicular component. The application of a strong in-plane field thus favors ϵ_Z and results in a smooth transition to a ferromagnetic (F) spin-ordered phase, which is distinctively metallic owing to the presence of gapless symmetry-protected edge states, with properties analogous to the ones of the quantum spin Hall (QSH) effect in two-dimensional topological insulators [10,11].

The critical point for the CAF-F transition is expected to be realized when the condition

$$\epsilon_Z(B_{\rm tot}) = 2|u_\perp(B_\perp)| \qquad (1)$$

is satisfied at some specific $B_\perp$-dependent value of the total field $B^*_{\rm tot}(B_\perp)$, at which the edge energy gap vanishes [8]. While compelling evidence of the CAF-F transition has been reported in Ref. [9] (and analogously in Ref. [12] also for single-layer graphene), the experimental observation of its critical point has not been reported so far. Here we individuate and analyze the critical point for the the CAF-F transition at the CNP in bilayer graphene. The data of the four-terminal resistance at CNP (R_{xx}^{CNP}) measured as a function of $B_{\rm tot}$ show a clear T-independent crossing point corresponding to the critical field $B^*_{\rm tot}$. By repeating the measurements at different fixed values of $B_\perp$, we show that $B^*_{\rm tot}$ scales linearly with $B_\perp$, which gives further evidence to the scenario of spin ordering at CNP governed by the ϵ_Z-$u_\perp$ competition and allows us to determine the energy scale of $u_\perp$ itself. The observation of the critical point also allowed us to conduct a successful scaling analysis on the data and determine a universal expression for R_{xx}^{CNP}.

The sample studied [see inset of Fig. 1(b)] is a van der Waals heterostructure consisting of a stacking of hexagonal boron nitride (h-BN) [13], bilayer graphene, and h-BN, produced using the pick-up technique described in Ref. [14] (an analogous sample with an additional top gate contact was studied in Ref. [9]). h-BN, acting as a high-quality dielectric substrate for graphene, allows high carrier mobility ($\mu \sim 5 \times 10^4$ cm^2 V^{-1} s^{-1}) [15]. We performed electrical transport measurements with a standard low-frequency (≈13 Hz) ac lock-in technique, using an excitation current of 100 nA and varying the carrier density with a back-gate contact. The sample was mounted on a holder with rotation capability, allowing us to vary the angle between the magnetic field and the graphene plane continuously from 0° to 180°. The correct orientation of the sample was tested after each modification of the angle by carefully checking the position of the integer quantum Hall plateaus at filling factor ±4, which depends on the $B_\perp$ component only. In addition, the sample was oriented so that the current was flowing parallel to the $B_\parallel$ component, avoiding orbital coupling due to the Lorentz force.

At $B_\parallel = 0$ T [Fig. 1(a)] the CNP is individuated as an intense maximum in R_{xx} close to $V_g = 0$ V. Divergent values of R_{xx}^{CNP} have been reported in works with ultraclean suspended samples [5]. In our supported bilayer graphene some residual

*sergio.pezzini@unipv.it

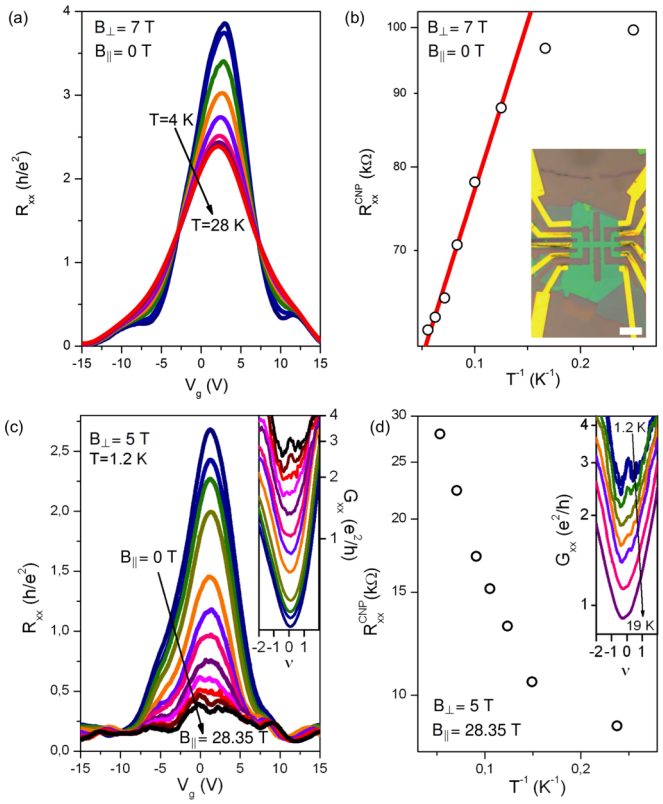

FIG. 1. (Color online) (a) R_{xx} as a function of V_g for increasing temperatures at $B_\perp = B_{\rm tot} = 7$ T. (b) Insulating T dependence of R_{xx}^{CNP}: the red line is a fit to $R_{xx}^{CNP} \propto \exp(\Delta/2k_BT)$. Inset: Optical microscopy image of the sample (the scale bar corresponds to 5 μm). (c) R_{xx} as a function of V_g for increasing $B_\parallel$ with fixed $B_\perp = 5$ T (see Ref. [16] for the values of $B_{\rm tot}$ and tilting angles), at $T \simeq 1.2$ K. Inset: G_{xx} as a function of the filling factor for the same values of $B_\parallel$. (d) Metallic T-dependence of R_{xx}^{CNP}. Inset: G_{xx} as a function of the filling factor for increasing temperatures in strong $B_\parallel$.

conductivity (possibly associated to charge puddles) is present even in this gapped phase, which is demonstrated by the clear thermally activated behavior shown in Fig. 1(b). Assuming that the resistance at the CNP follows $R_{xx}^{CNP} \propto \exp(\Delta/2k_BT)$, we estimated an amplitude $\Delta = 10.7 \pm 0.4$ K for the energy gap at $B_\perp = 7$ T. While such insulating behavior at the CNP is not enough to distinguish the CAF phase from the other gapped ground states (as the fully and partially layer polarized), it is the evolution of the transport properties with strong $B_\parallel$ which demonstrates the CAF order and its transition to the F phase. Figure 1(c) shows the evolution of R_{xx} as a function of V_g when a strong $B_\parallel$ is applied in addition to the quantizing $B_\perp$: as $B_\parallel$ increases, R_{xx}^{CNP} drops dramatically. In the inset we show that a highly conductive state is induced at $\nu = 0$, with G_{xx}^{CNP} approaching $4e^2/h$, which is the expected value for a four-probe measurement of the conductance in the F phase. The not-exact quantization detected in our measurements (also observed in Refs. [9,17,18]) indicates residual backscattering likely due to short circuiting via bulk states and/or nonideal contacts acting as uncontrolled decoherence sites [17]. In addition to the quantization of G_{xx}^{CNP}, the F phase is identified as the only metallic ground state, owing to its gapless edge excitation [3]: the metallic T dependence of the CNP in strong $B_\parallel$ is clearly shown in Fig. 1(d). The $B_\parallel$-driven insulator-to-metal transition at the CNP here described does not show sudden changes in the transport properties (see the smooth traces in Fig. 2), as expected only for the CAF-F transition [3]. Moreover, the gap of the insulating phase gradually closes upon the application of increasing $B_\parallel$ [see Fig. 3(c)]. All these elements together demonstrate the realization of a CAF-F phase transition at CNP in bilayer graphene, completely analogous to the one reported in Ref. [9].

In order to individuate the critical field for the CAF-F transition demonstrated by the previous data, we measured R_{xx}^{CNP} at different values of T and $B_{\rm tot}$, while keeping $B_\perp$ constant. This is done in order to keep the anisotropy energy $u_\perp$ unchanged while increasing ϵ_Z and thus driving the transition. A T-independent crossing point for the isotherms of R_{xx}^{CNP} is clearly visible in each panel of Fig. 2 (each of them showing data acquired at a single value $B_\perp = 4$, 5, 6, and 7 T). These data provide experimental identification of the critical point for the CAF-F phase transition at CNP in bilayer graphene. In the insulating phase, the values of R_{xx}^{CNP} clearly increase with $B_\perp$, in accordance with previous observations [5,6]; on the other hand, R_{xx}^{CNP} does not depend on $B_\perp$ in the metallic F phase [see Fig. 3(a)]. This indicates that the gap of the CAF phase increases with $B_\perp$, while the system becomes insensitive

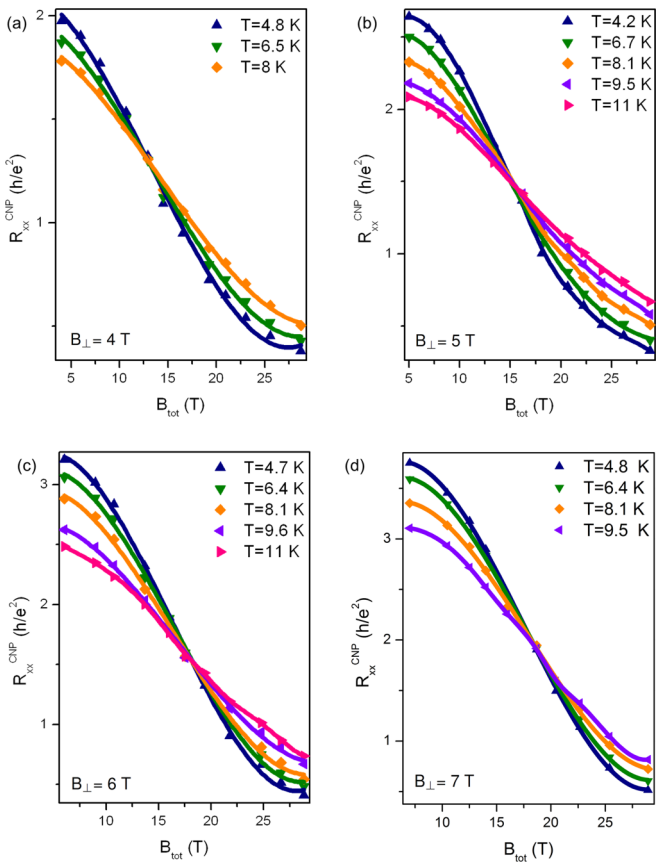

FIG. 2. (Color online) Isotherms of R_{xx} in correspondence of the CNP as a function of $B_{\rm tot}$ with increasing perpendicular components: (a) $B_\perp = 4$ T, (b) $B_\perp = 5$ T, (c) $B_\perp = 6$ T, and (d) $B_\perp = 7$ T. The symbols correspond to the experimental points, while the continuous lines are obtained by interpolation with grade-five polynomials.

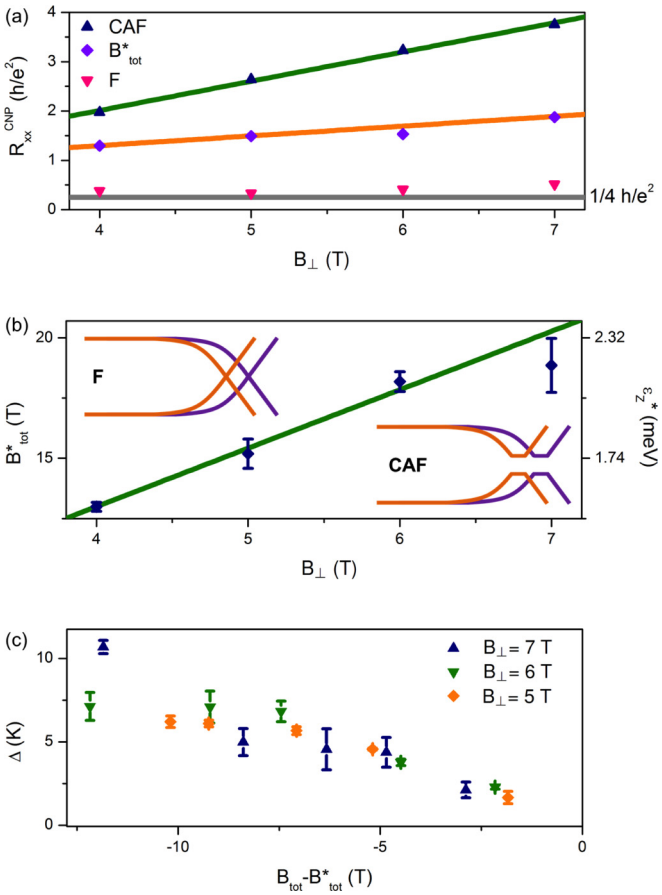

FIG. 3. (Color online) (a) R_{xx}^{CNP} as a function of $B_\perp$ at $B_\parallel = 0$ T (CAF, blue up triangles), with the largest $B_\parallel$ applied (F, pink down triangles) and at the critical point ($B_{\rm tot}^*$, violet diamonds), at $T \approx 4.5$ K. The green line is a guide to the eye, the gray one indicates $\frac{1}{4}h/e^2$, and the orange one is $A(B_\perp)$ (see text). (b) Critical total field ($B_{\rm tot}^*$, left axis) and critical Zeeman energy (ϵ_Z^*, right axis) for the CAF-F transition as a function of $B_\perp$. The data points are calculated as mean values of $B_{\rm tot}$ at the T-independent crossings of the solid lines in Fig. 2, while the error bars correspond to one standard deviation. Inset: The bulk and edge energy spectrum of the CAF and F phases are sketched on the two sides of the phase boundary. (c) Energy gap Δ as a function of $B_{\rm tot} - B_{\rm tot}^*$, estimated from the thermally activated R_{xx}^{CNP} in the CAF phase for different $B_\perp$.

to $B_\perp$ once the F order is realized (the small deviations in the data at $B_\perp = 6$, 7 T should become negligible if higher $B_{\rm tot}$ could be reached with our experimental system).

The values of critical field $B_{\rm tot}^*$ corresponding to the T-independent crossing points are plotted in Fig. 3(b) as a function of $B_\perp$. It is clearly shown that $B_{\rm tot}^*$ increases with $B_\perp$ and a linear dependence can be inferred. From a linear fit to the data [see green line in Fig. 3(b)], we obtain

$$B_{\rm tot}^* = (2.42 \pm 0.21) \times B_\perp. \qquad (2)$$

Equation (2) represents the first experimental determination of the $B_\perp$ dependence for this critical field. If we consider the condition expressed by Eq. (1), we get an estimate for the anisotropy energy $u_\perp = (1.62 \pm 0.14)$ K/T $\times B_\perp$ (assuming $g = 2$), in accordance with the prediction of Refs. [3,8] ($u_\perp \approx$ 1–10 K/T$\times B_\perp$). The Zeeman energies at the critical points ϵ_Z^* [see right axis in Fig. 3(b)] are consistent with the CAF-F boundary $\epsilon_Z \approx 0.8$ meV reported in Ref. [9] for $B_\perp = 1.75$ T, which has been estimated on the basis of the saturation of R_{xx}^{CNP} rather than at the insulator-to-metal transition as done in the present work. The reliability of our estimation of the critical point is further evidenced by the evolution of the energy gap Δ of the insulating phase as the in-plane field is increased. In Fig. 3(c) we show that Δ [obtained by fitting the thermally activated resistance as in Fig. 1(b)] continuously decreases towards $B_{\rm tot} = B_{\rm tot}^*$, eventually pointing at vanishing values, perfectly matching the evolution of the edge gap described in Ref. [8].

A distinctive feature of the phase transitions in quantum systems is represented by the scaling of physical observables in the vicinity of the critical point at finite temperature [19]. In the following we individuate a scaling law for the CAF-F transitions observed at different $B_\perp$ and determine a universal expression for R_{xx}^{CNP}. Figure 4(a) shows the same data of R_{xx}^{CNP} as in Figs. 2(a)–2(d), plotted as a function of $(B_{\rm tot} - B_{\rm tot}^*)/T$. The data relative to the four values of $B_\perp$ collapse into four different curves, demonstrating a nearly ideal scaling of R_{xx}^{CNP} with $(B_{\rm tot} - B_{\rm tot}^*)/T$. The four curves coincide for $B_{\rm tot} \gg B_{\rm tot}^*$, where R_{xx}^{CNP} has been shown to be a $B_\perp$-independent quantity, while they differ in the vicinity of the transition ($B_{\rm tot} \approx B_{\rm tot}^*$) and in the CAF region ($B_{\rm tot} \ll B_{\rm tot}^*$). For $B_{\rm tot} \approx B_{\rm tot}^*$, linearity is observed in the four curves. Our best estimate gives an intercept $A(B_\perp) = 1.31 \times 10^4 + 5.1 \times 10^3 B_\perp$ (T) Ω, together with a slope $S(B_\perp) = 9.33 \times 10^3 + 1.25 \times 10^3 B_\perp$ (T) Ω K/T, which apply for any of the $B_\perp$ values. These two parameters can therefore be inserted into a tentative general expression for R_{xx}^{CNP} in the vicinity of the transition:

$$R_{xx}^{CNP}(B_{\rm tot}, B_\perp, T) = A(B_\perp) + S(B_\perp)\left(\frac{B_{\rm tot} - B_{\rm tot}^*(B_\perp)}{T}\right). \qquad (3)$$

The universality of Eq. (3) is demonstrated in Fig. 4(b), where $(R_{xx}^{CNP} - A(B_\perp))/S(B_\perp)$ is plotted as a function of $(B_{\rm tot} - B_{\rm tot}^*)/T$ and our whole experimental data set collapses into a unique curve [as expected, Eq. (3) does not apply

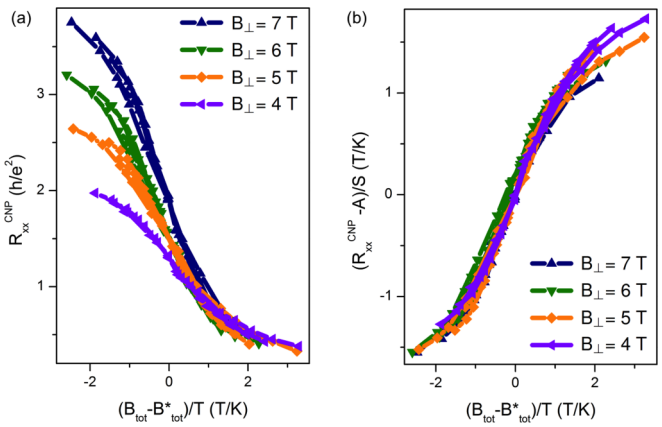

FIG. 4. (Color online) (a) R_{xx}^{CNP} as a function of $(B_{\rm tot} - B_{\rm tot}^*)/T$ for the four values of $B_\perp$ considered: scaling behavior is clearly shown. (b) $(R_{xx}^{CNP} - A(B_\perp))/S(B_\perp)$ as a function of $(B_{\rm tot} - B_{\rm tot}^*)/T$, demonstrating the universality of the relation expressed by Eq. (3).

in the region $B_{\rm tot} \gg B^*_{\rm tot}$, where no dependence on $B_\perp$ has already been pointed out]. The parameter $A(B_\perp)$ corresponds to the value of R_{xx}^{CNP} at the critical field. The fact that $R_{xx}^{CNP}(B^*_{\rm tot})$ is a $B_\perp$-dependent quantity is distinctive of this transition with respect to, e.g., liquid-to-insulator transitions in two-dimensional electron gases [20] (where a universal value of the resistance is found at the critical point), and once more points out the role of the anisotropy energy $u_\perp$.

In conclusion, we performed magnetotransport measurements on high-mobility bilayer graphene enclosed by h-BN, making use of tilted magnetic fields. We found clear evidence of a transition from an insulating to a metallic state at the CNP, driven by the application of a strong in-plane field and consistent with a CAF-F spin phase transition. We showed that a critical point for this transition can be individuated, corresponding to a T-independent crossing for the isotherms of the four-probe resistance, and we obtained a linear dependence for the critical field as a function of the perpendicular component. The value of the four-probe resistance at the transition is found to depend on the perpendicular component of the field, which determines the strength of the interaction-induced anisotropy. In the vicinity of the transition we demonstrated scaling behavior for the resistance and we proposed a universal expression as a function of total magnetic field, perpendicular component, and temperature. The latter findings of our analysis encourage further theoretical work on the subject.

We acknowledge Dr. Niko Tombros for providing the sample and for enlightening discussions. This work has been supported by the following projects: JCYL SA226U13, FPU AP2009-2619, MINECO MAT2013-46308-C2-1-R, and European Union CTA-228043-EuroMagNET II Programme.

[1] E. McCann and V. I. Falko, Phys. Rev. Lett. **96**, 086805 (2006).
[2] K. S. Novoselov, E. McCann, S. V. Morozov, V. I. Fal'ko, M. I. Katsnelson, U. Zeitler, D. Jiang, F. Schedin, and A. K. Geim, Nat. Phys. **2**, 177 (2006).
[3] M. Kharitonov, Phys. Rev. Lett. **109**, 046803 (2012).
[4] J. Velasco Jr., L. Jing, W. Bao, Y. Lee, P. Kratz, V. Aji, M. Bockrath, C. N. Lau, C. Varma, R. Stillwell, D. Smirnov, Fan Zhang, J. Jung, and A. H. MacDonald, Nat. Nanotechnol. **7**, 156 (2012).
[5] B. E. Feldman, J. Martin, and A. Yacoby, Nat. Phys. **5**, 889 (2009).
[6] F. Freitag, J. Trbovic, M. Weiss, and C. Schonenberger, Phys. Rev. Lett. **108**, 076602 (2012).
[7] R. T. Weitz, M. T. Allen, B. E. Feldman, J. Martin, and A. Yacoby, Science **330**, 812 (2010).
[8] M. Kharitonov, Phys. Rev. B **86**, 075450 (2012).
[9] P. Maher, C. R. Dean, A. F. Young, T. Taniguchi, K. Watanabe, K. L. Shepard, J. Hone, and P. Kim, Nat. Phys. **9**, 154 (2013).
[10] C. L. Kane and E. J. Mele, Phys. Rev. Lett. **95**, 146802 (2005).
[11] M. Z. Hasan and E. J. Mele, Rev. Mod. Phys. **82**, 3045 (2010).
[12] A. F. Young, J. D. Sanchez-Yamagishi, B. Hunt, S. H. Choi, K. Watanabe, T. Taniguchi, R. C. Ashoori, and P. Jarillo-Herrero, Nature (London) **505**, 528 (2014).
[13] C. R. Dean, A. F. Young, I. Meric, C. Lee, L. Wang, S. Sorgenfrei, K. Watanabe, T. Taniguchi, P. Kim, K. L. Shepard, and J. Hone, Nat. Nanotechnol. **5**, 722 (2010).
[14] P. J. Zomer, M. H. D. Guimarães, J. C. Brant, N. Tombros, and B. J. van Wees, Appl. Phys. Lett. **105**, 013101 (2014).
[15] C. Cobaleda, S. Pezzini, E. Diez, and V. Bellani, Phys. Rev. B **89**, 121404(R) (2014).
[16] Total fields $B_{\rm tot}$ and tilting angles of the sample θ for the traces in Fig. 1(c) (from navy to black): $B_{\rm tot} = 5$ T, $\theta = 0°$; $B_{\rm tot} = 6.95$ T, $\theta = 44°$; $B_{\rm tot} = 8.12$ T, $\theta = 52°$; $B_{\rm tot} = 10$ T, $\theta = 60°$; $B_{\rm tot} = 13.35$ T, $\theta = 68°$; $B_{\rm tot} = 16.18$ T, $\theta = 72°$; $B_{\rm tot} = 18.14$ T, $\theta = 74°$; $B_{\rm tot} = 20.67$ T, $\theta = 76°$; $B_{\rm tot} = 22.23$ T, $\theta = 77°$; $B_{\rm tot} = 24.05$ T, $\theta = 78°$; $B_{\rm tot} = 26.2$ T, $\theta = 79°$; and $B_{\rm tot} = 28.8$ T, $\theta = 80°$.
[17] A. Roth, C. Brüne, H. Buhmann, L. W. Molenkamp, J. Maciejko, X.-L. Qi, and S.-C. Zhang, Science **325**, 294 (2009).
[18] M. König, S. Wiedmann, C. Brÿne, A. Roth, H. Buhmann, L. W. Molenkamp, X.-L. Qi, and S.-C. Zhang, Science **318**, 766 (2007).
[19] S. Sachdev, *Quantum Phase Transitions*, 2nd ed. (Cambridge University Press, Cambridge, UK, 2011).
[20] D. Shahar, D. C. Tsui, M. Shayegan, R. N. Bhatt, and J. E. Cunningham, Phys. Rev. Lett. **74**, 4511 (1995).